Supplementary Information

Molecular insights into a distinct class of terpenoid cyclases

Siyu Li[1,3], Jian-Wen Huang[1,2,3], Jian Min[1], Hao Li[1], Meidan Ning[1], Shuyu Zhou[1], Yu Yang[1]*, Chun-Chi Chen[1,2]*, Rey-Ting Guo[1,2]*

[1]State Key Laboratory of Biocatalysis and Enzyme Engineering, Hubei Hongshan Laboratory, School of Life Sciences, Hubei University, Wuhan 430062, PR China

[2]Zhejiang Key Laboratory of Medical Epigenetics, Department of Immunology and Pathogen Biology, School of Basic Medical Sciences, Hangzhou Normal University, 311121, Hangzhou, China

[3]These authors contributed equally

*Corresponding authors. E-mail addresses: yangyu@hubu.edu.cn (Y. Yang), guoreyting@hubu.edu.cn (R.-T. Guo), ccckate0722@hubu.edu.cn (C.-C. Chen).

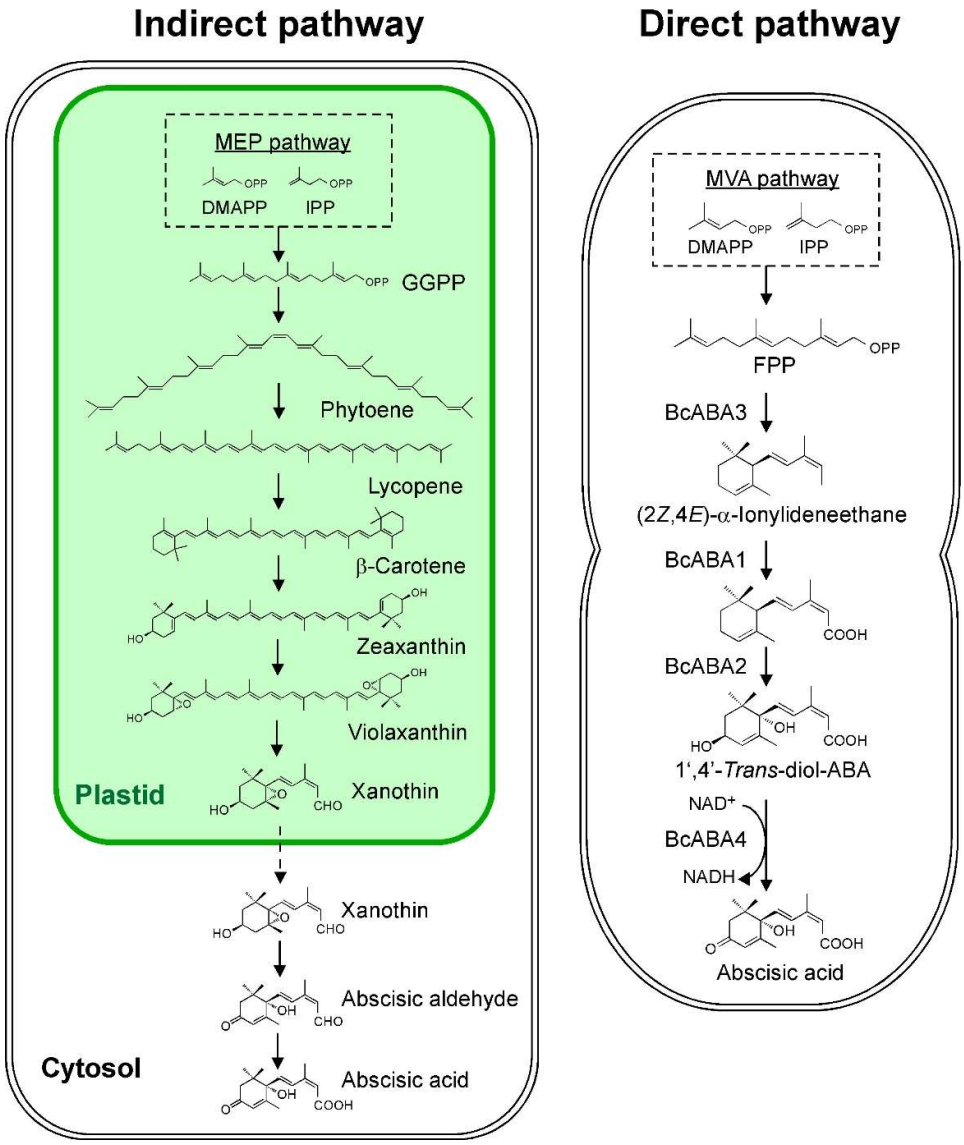

Supplementary Fig. 1. ABA biosynthesizing pathways. The indirect and direct ABA biosynthetic pathway in plants (left) and an ABA-producing fungus *Botrytis cinerea* (right), respectively, are depicted. DMAPP, dimethylallyl pyrophosphate; IPP, isopentenyl pyrophosphate; GGPP, geranylgeranyl pyrophosphate; FPP, farnesyl pyrophosphate.

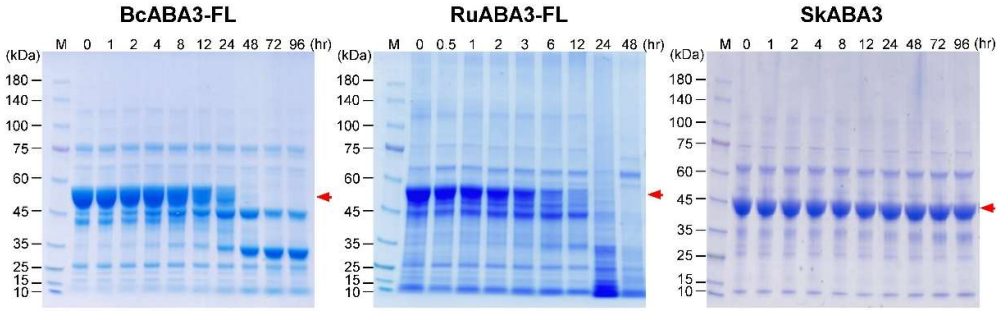

Supplementary Fig. 2. Stability analysis of recombinant ABA3 proteins. Recombinant proteins of BcABA3-FL, RuABA3-FL and SkABA3 were analyzed by SDS-PAGE after incubated at the crystallization temperature for indicated period of time. Red arrows indicate the expected position of the full-length proteins. M, marker. The uncropped scans of all gels are provided as a Source Data file.

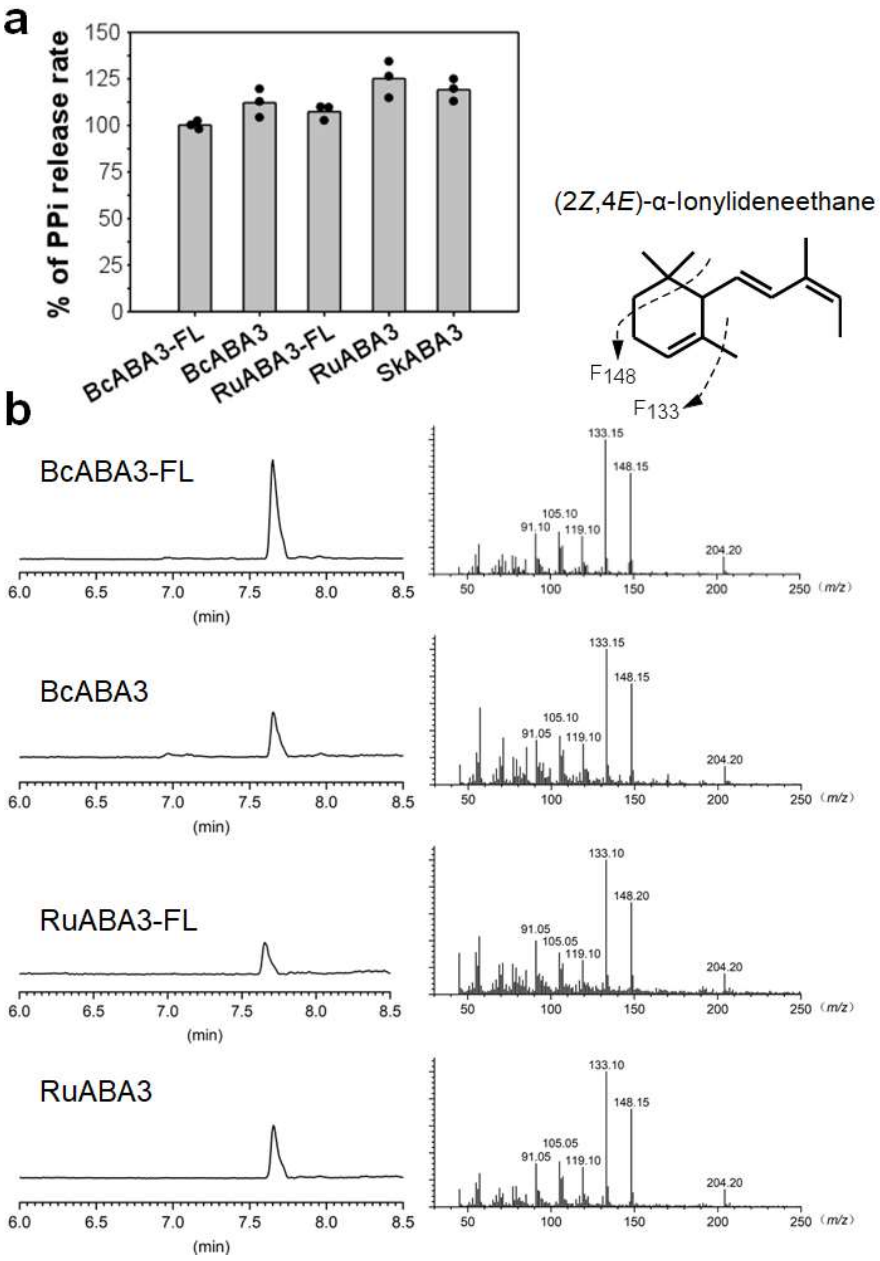

Supplementary Fig. 3. Activity assessment of ABA3 proteins. (**a**) The PPi release rate of full-length and N-terminus truncated BcABA3, RuABA3 and SkABA3 when using FPP as a substrate, and the relative activities of each sample were presented as percentages of BcABA3-FL. The individual and average values of each sample in the triplicate assay were presented in dots and bars, respectively. (**b**) The reaction products of full-length and N-terminus truncated BcABA3 and RuABA3 were analyzed by GC-MS. The GC-MS chromatograms (left panel, *m*/*z* 133 and 148) MS spectra (right panel) of reaction product of each enzyme are displayed. Note that the intact (*m*/*z*, 204.20) and two main fragment ions (*m*/*z*, 148.1 and 133.1) resulted from a retro-Diels-Alder fragmentation of (2*Z*,4*E*)-α-ionylideneethane as previously described can be identified in both enzyme reactions[1]. Source data are provided as a Source Data file

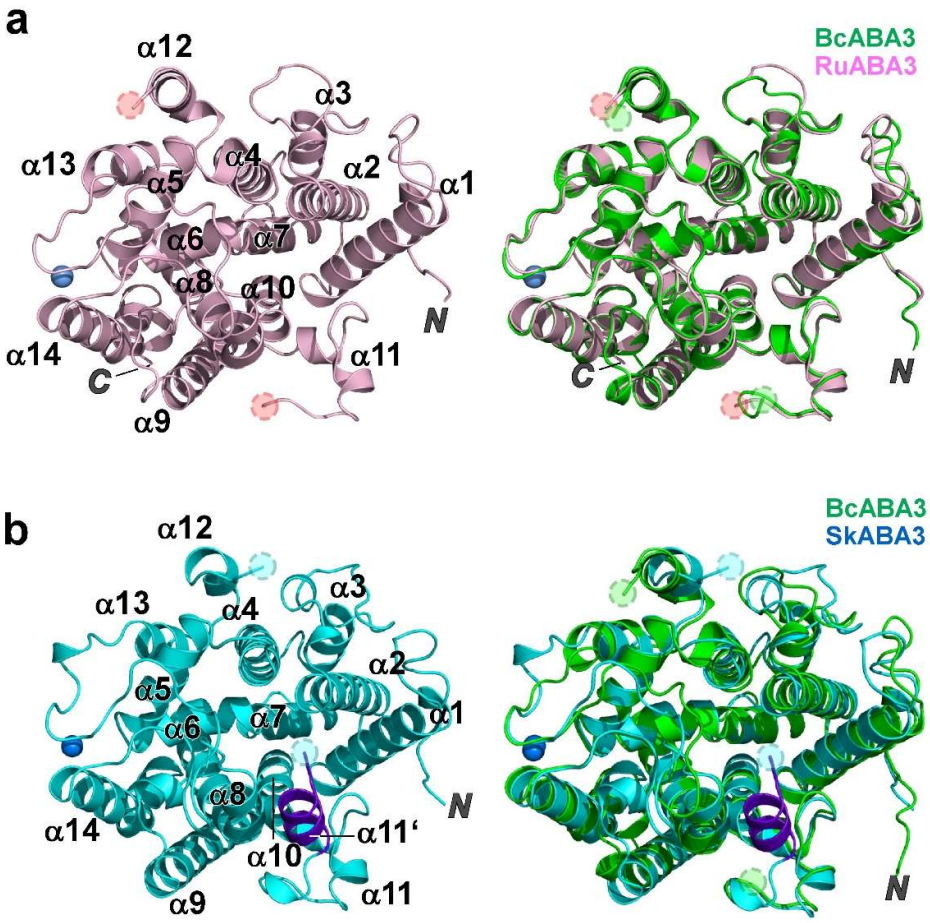

Supplementary Fig. 4. Overall structure of RuABA3 and SkABA3. The overall structures of (**a**) RuABA3 and (**b**) chain A in the apo-SkABA3 structure are displayed in cartoon model. The helix labeling, metal ion and the breaking points on helix α11, α11' and α12 are indicated as in **Fig. 1b**. Right panels are structural superimposition of BcABA3 (green).

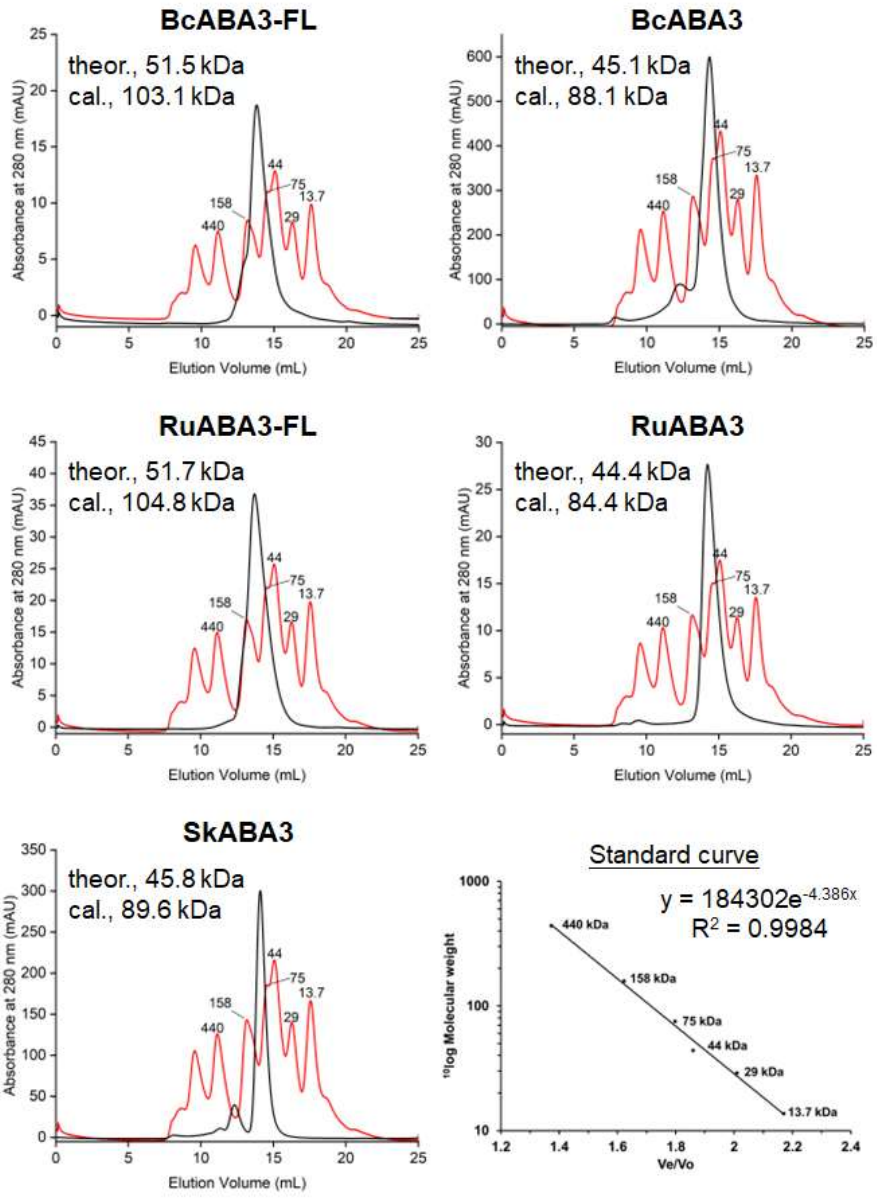

Supplementary Fig. 5. Size exclusion chromatographic (SEC) analyses of ABA3 proteins. Red and black lines represent the chromatogram trace of standard protein markers and recombinant protein of each ABA3, respectively. The theoretical molecular weight of the single polypeptide of individual protein (theor.) and the molecular mass in solution calculated from the standard curve (cal.) are shown in each panel.

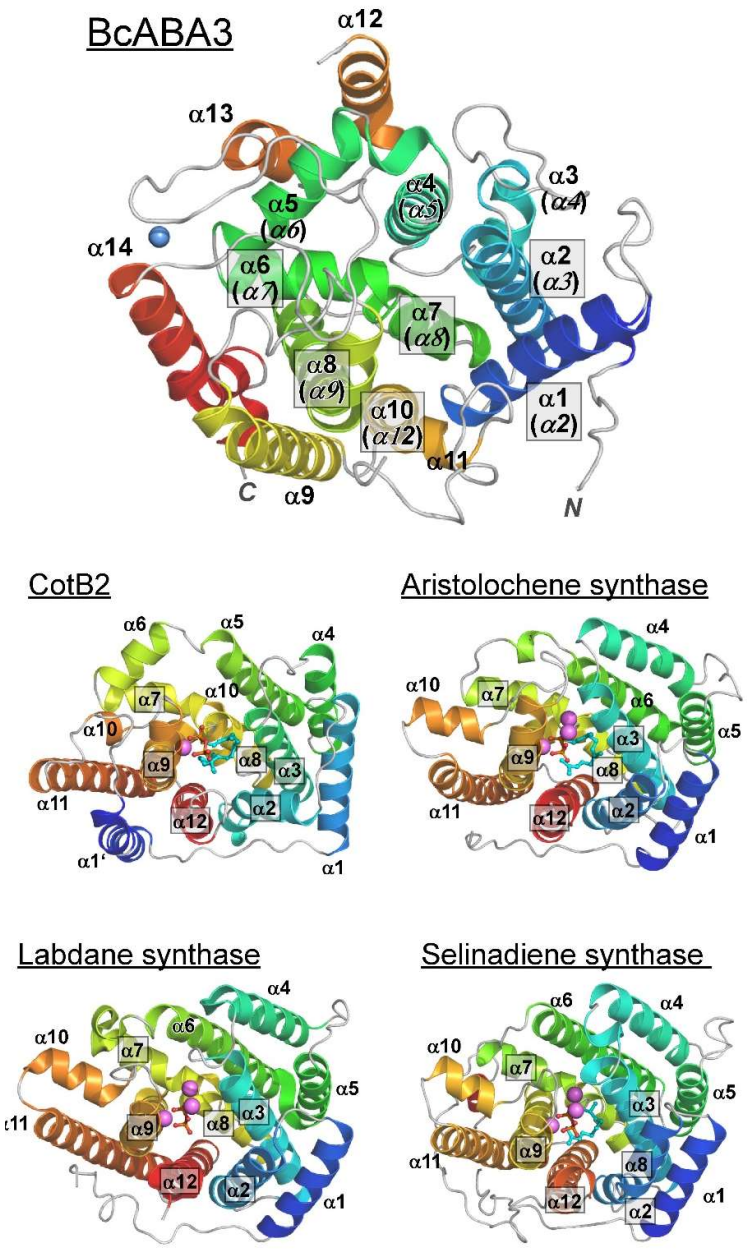

Supplementary Fig. 6. Homologous structures of BcABA3. The cartoon models of apo-BcABA3 (PDB ID, 8ZAC [http://doi.org/10.2210/pdb8ZAC/pdb]), CotB2 from *Streptomyces melanosporofaciens* (PDB ID, 5GUE; GGPP cyclase [http://doi.org/10.2210/pdb5GUE/pdb]), aristolochene synthase from *Aspergillus terreus* (PDB ID, 4KUX; FPP cyclase [http://doi.org/10.2210/pdb4KUX/pdb]), labdane synthase from *Streptomyces* sp. (PDB ID, 6OH6; GGPP cyclase [http://doi.org/10.2210/pdb6OH6/pdb]) and selinadiene synthase from *S. pristinaespiralis* (PDB ID, 4OKZ; FPP cyclase [http://doi.org/10.2210/pdb4OKZ/pdb]). The helices that construct substrate-binding pocket in all TCs and their equivalents in BcABA3 are framed. In BcABA3, the labels of the counterparts of each helix in TCs

are also shown below in italics. The Zn^{2+} and Mg^{2+} ions are shown in cyan and violet spheres and the bound ligands are in sticks.

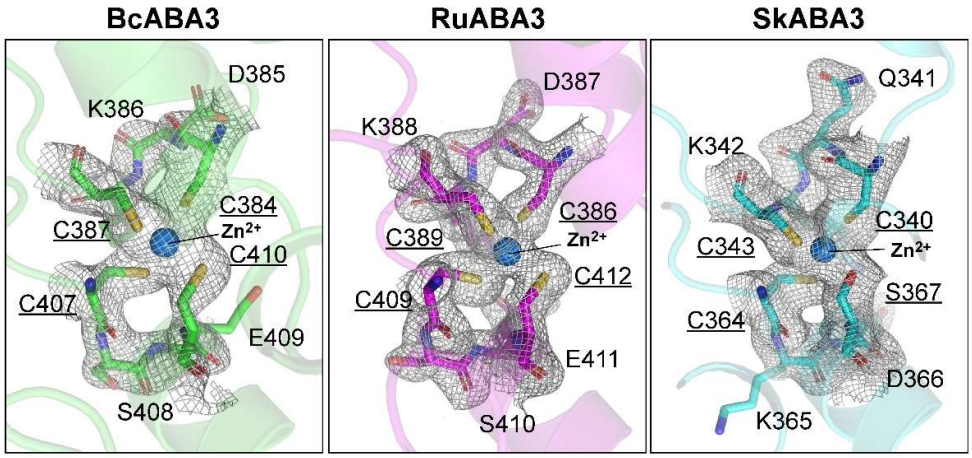

Supplementary Fig. 7. Electron density maps of Zn^{2+} ion-binding motif in the ABA3 structures. The $2F_o$-F_c electron density maps of residues that comprise the Zn^{2+} ion-binding motifs along with the metal ions in apo-BcABA3 (PDB ID, 8ZAC [http://doi.org/10.2210/pdb8ZAC/pdb]), apo-RuABA3 (PDB ID, 8ZAD [http://doi.org/10.2210/pdb8ZAD/pdb]) and apo-SkABA3 (PDB ID, 8ZAF [http://doi.org/10.2210/pdb8ZAF/pdb]) are contoured at 1.0 σ and shown in mesh. The metal ions and protein residues are shown in spheres and sticks, respectively. The Zn^{2+} ion-coordinating residues are labeled by underlined characters.

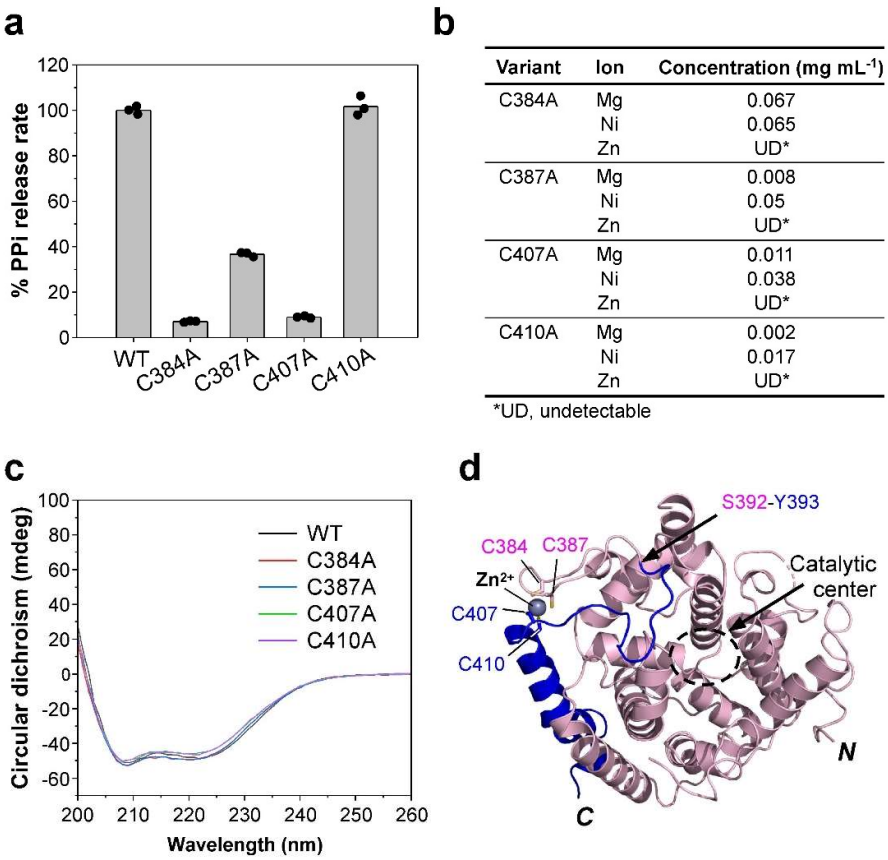

Supplementary Fig. 8. The role of the Zn^{2+} ion-binding residues in BcABA3. The (**a**) PPi release rate, (**b**) atomic spectrometric analyses and (**c**) CD analyses of wild type and variants with the Zn^{2+}-coordinating residues substituted with Ala. (**d**) The cartoon model of the apo-form BcABA3 with the Zn^{2+} ion-coordinating residues and Zn^{2+} ion respectively labeled by sticks and a sphere. The region and residues colored in blue are absent in bcABA3-S, a natural variant of BcABA3 that does not produce (2*Z*,4*E*)-α-ionylideneethane. The central cavity that accounts for the catalytic center is indicated by the dashed circle. The N- and C-terminus of the polypeptide are indicated. Source data of **8a** are provided as a Source Data file.

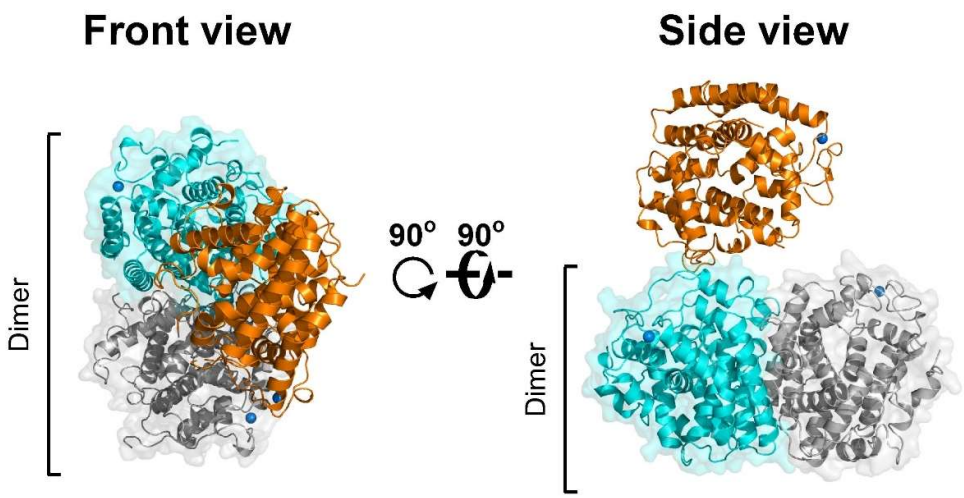

Supplementary Fig. 9. Three polypeptide chains in the apo-SkABA3 crystal. Two views of the three polypeptide chains in an asymmetric unit of the apo-SkABA3 crystal structure (PDB ID, 8ZAF [http://doi.org/10.2210/pdb8ZAF/pdb]) are presented in cyan, gray and orange cartoon models. The two that form a homodimer (cyan and gray) in the same configuration as BcABA3 and RuABA3 are noted.

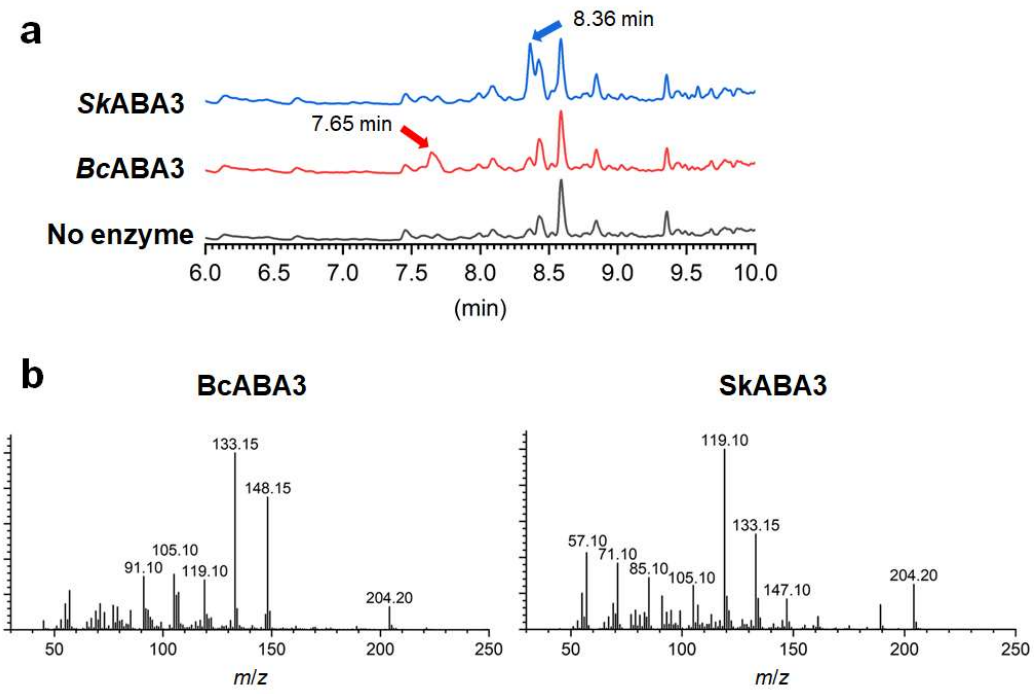

Supplementary Fig. 10. GS-MS analyses of the reaction product of SkABA3. (**a**) The total ion chromatograms of FPP converted by SkABA3 (blue trace) and BcABA3 (red trace). (**b**) The mass spectra of (2*Z*,4*E*)-α-ionylideneethane produced by BcABA3 (7.65 min) and the main peak in the reaction mixture catalyzed by SkABA3 (8.36 min). Source data of **10a** are provided as a Source Data file.

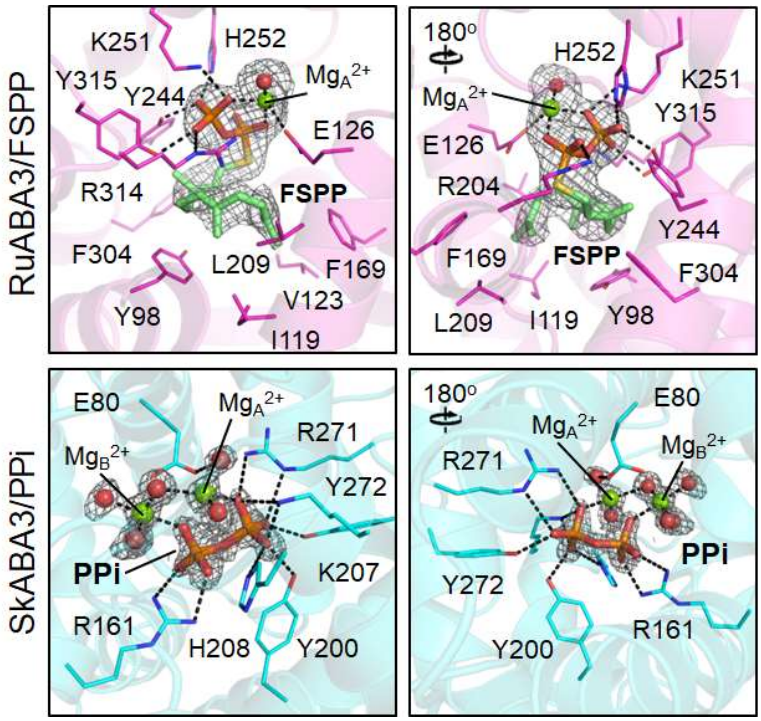

Supplementary Fig. 11. The omit maps of ligands bound in the RuABA3 and SkABA3 complex structures. The enzyme-ligand interaction networks in the complex structures RuABA3/FSPP (PDB ID, 8ZAE [http://doi.org/10.2210/pdb8ZAE/pdb]) and SkABA3/PPi (PDB ID, 8ZAG [http://doi.org/10.2210/pdb8ZAG/pdb]) are depicted as described in **Fig. 2**. The F_o-F_c polder omit maps of FSPP, PPi, Mg^{2+} ions and coordinating waters contoured at 3.0 σ are shown in mesh. Two views relative at the Y-axis by 180° are presented. Dashed lines indicate distance < 3.5 Å.

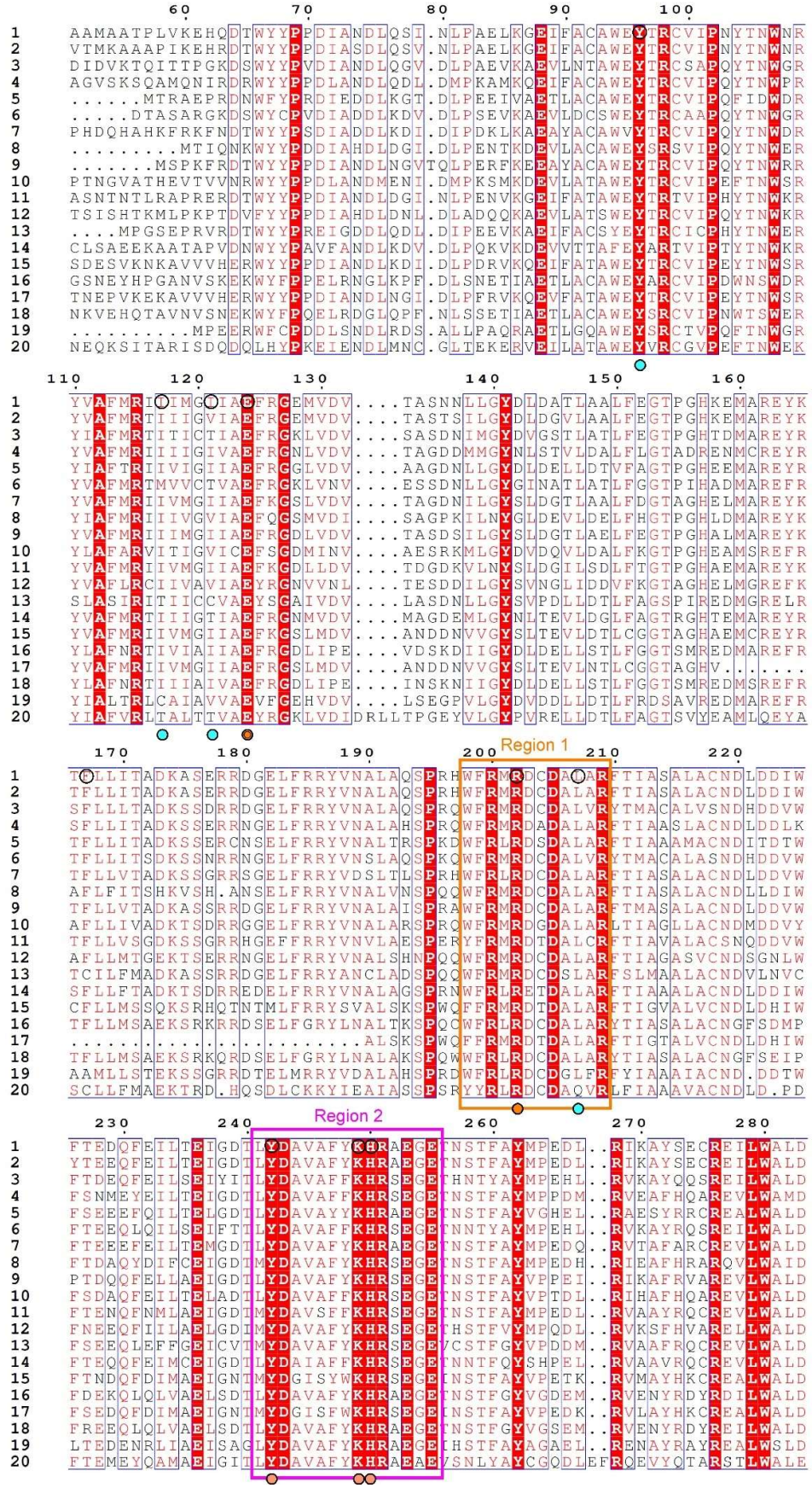
Region 1
Region 2

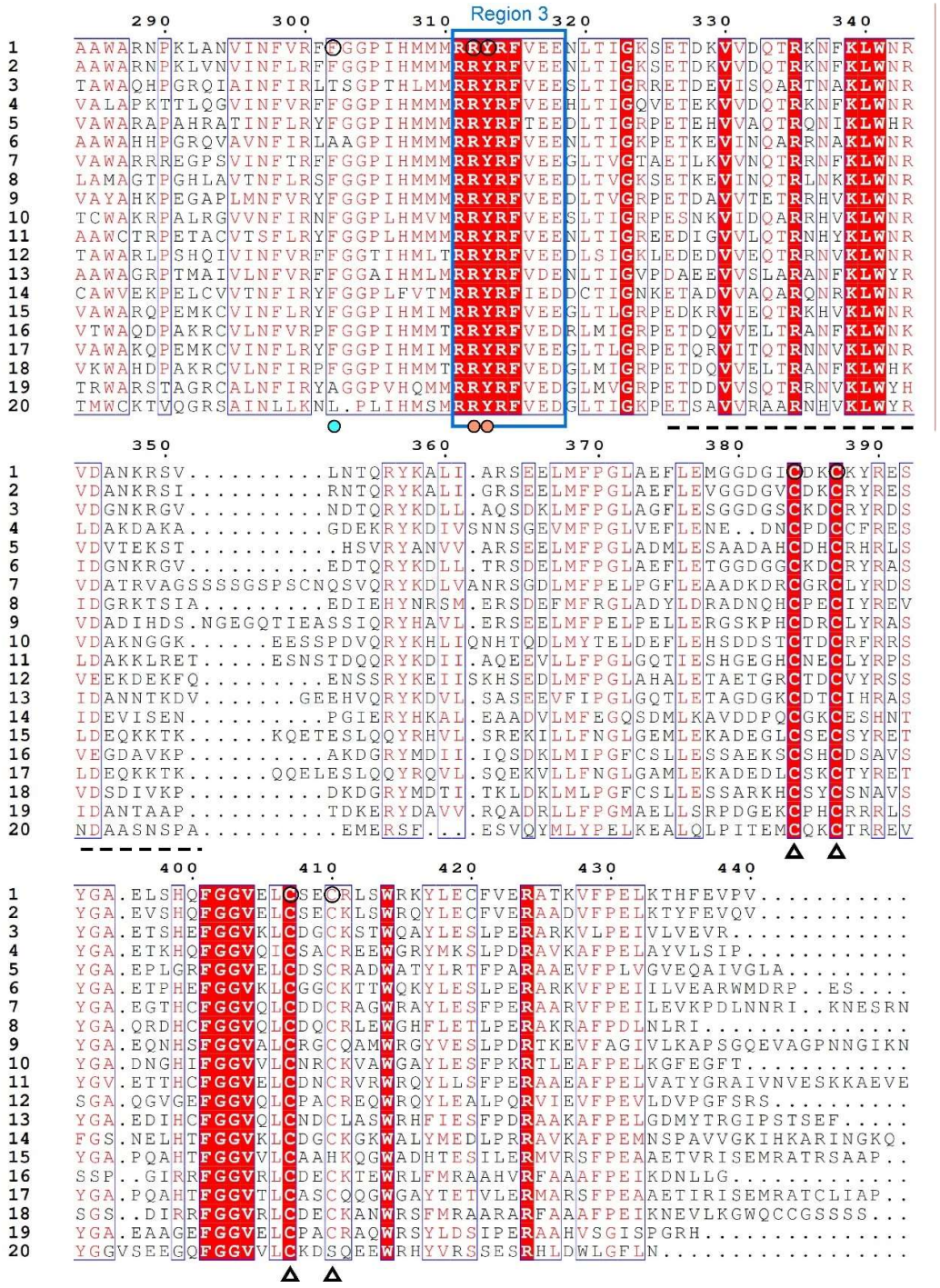

Supplementary Fig. 12. Partial protein sequence alignment of BcABA3 and homologues. Sequences that share 36.3-86.2% identity to BcABA3 were aligned by Clustal Omega[2], and the graph was produced by Espript 3.0[3]. Three conserved regions proposed by Takino et al. are boxed[1]; residues that interact with PPi and hydrocarbon moiety are marked by orange and blue dots, respectively; the missing fragment in the apo-form ABA3 structures is denoted by a dashed line under the alignment; four Zn-coordinating residues are indicated by triangles. The residues of BcABA3 subjected to

mutagenesis experiments are circles. The protein sequences used in this alignment are listed in **Supplementary Table 7**.

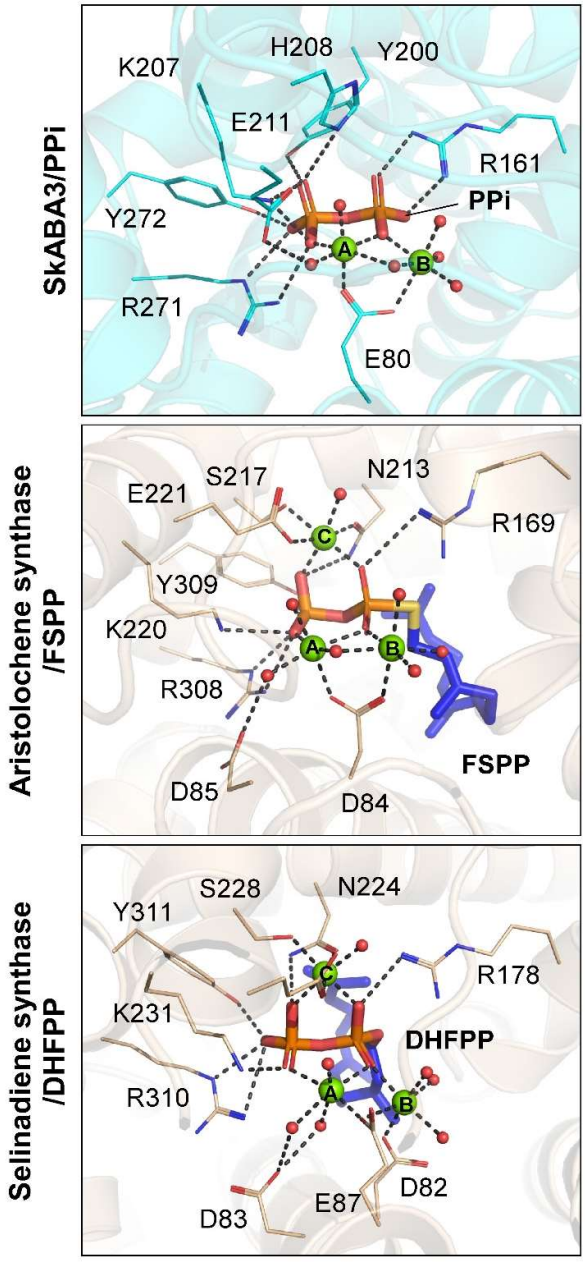

Supplementary Fig. 13. PPi interaction networks of TCs. The PPi-enzyme interaction networks in SkABA3/PPi (PDB ID, 8ZAG [http://doi.org/10.2210/pdb8ZAG/pdb]), aristolochene/FSPP (PDB ID, 4KUX [http://doi.org/10.2210/pdb4KUX/pdb]) and selinadiene synthase/DHFPP (PDB ID, 4OKZ [http://doi.org/10.2210/pdb4OKZ/pdb]) are depicted. The bound ligands and protein residues are shown in sticks and lines, respectively. Three Mg ions are labeled alphabetically and metal ion-coordinating waters are shown in red spheres. Polar interactions with distance < 3.5 Å are shown by dashed lines. DHFPP, dihydrofarnesyl pyrophosphate.

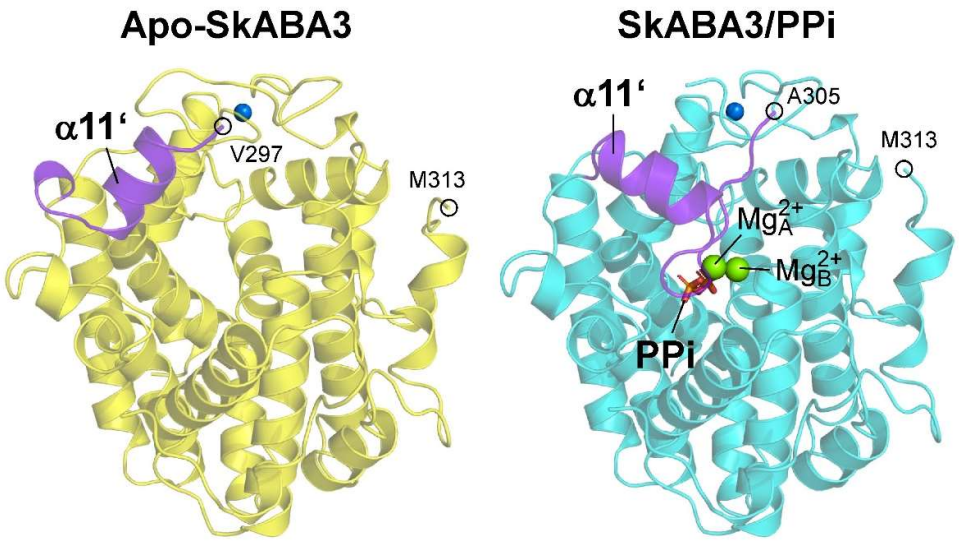

Supplementary Fig. 14. Active site conformational change in SkABA3. The overall structure of apo-SkABA3 (PDB ID, 8ZAF [http://doi.org/10.2210/pdb8ZAF/pdb]) and SkABA3/PPi (PDB ID, 8ZAG [http://doi.org/10.2210/pdb8ZAG/pdb]) are presented as those in **Fig. 2a**. Helix α11’ and the following loop are indicated and colored in purple. Circles indicate the either ends on the missing fragment in both structures. Note that helix α11’ turns 90° and reorients toward the substrate-binding pocket in the SkABA3/PPi complex.

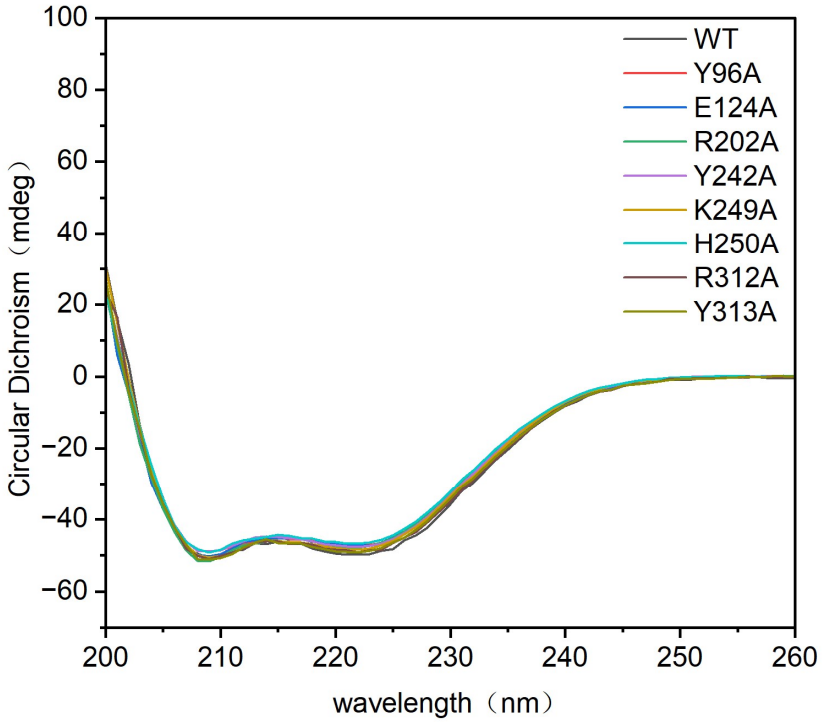

Supplementary Fig. 15. CD spectra of wild type and variant BcABA3 proteins.

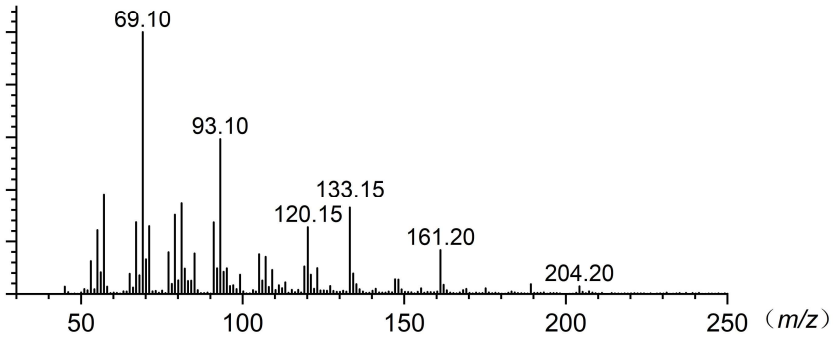

Supplementary Fig. 16. The mass spectrum of (*E*)-β-farnesene.

Supplementary Tables

Supplementary Table 1. Amino acid sequences of ABA3 proteins involved in this study

Protein sequence
BcABA3-FL (GenBank No., XP_024550392.1) HHHHHHENLYFQGAGAGAGAGAGMQQVITQTLVDDRFIQISDSKKSEGLATDSTKRQS QEQPIHDKDPIKAATAAMAATPLVKEHQDTWYYPPDIANDLQSINLPAELKGEIFACAW EYTRCVIPNYTNWNRYVAFMRIIIMGIIAEFRGEMVDVTASNNLLGYDLDATLAALFEG TPGHKEMAREYKTFLLITADKASERRDGELFRRYVNALAQSPRHWFRMRDCDALARF TIASALACNDLDDIWFTEDQFEILTEIGDTLYDAVAFYKHRAEGETNSTFAYMPEDLRIK AYSECREILWALDAAWARNPKLANVINFVRFFGGPIHMMMRRYRFVEENLTIGKSETDK VVDQTRKNFKLWNRVDANKRSVLNTQRYKALIARSEELMFPGLAEFLEMGGDGICDK CKYRESYGAELSHQFGGVELCSECRLSWRKYLECFVERATKVFPELKTHFEVPV
BcABA3 HHHHHHENLYFQGAGAGAGAGAGAKEHQDTWYYPPDIANDLQSINLPAELKGEIFAC AWEYTRCVIPNYTNWNRYVAFMRIIIMGIIAEFRGEMVDVTASNNLLGYDLDATLAALF EGTPGHKEMAREYKTFLLITADKASERRDGELFRRYVNALAQSPRHWFRMRDCDALA RFTIASALACNDLDDIWFTEDQFEILTEIGDTLYDAVAFYKHRAEGETNSTFAYMPEDLRI KAYSECREILWALDAAWARNPKLANVINFVRFFGGPIHMMMRRYRFVEENLTIGKSETD KVVDQTRKNFKLWNRVDANKRSVLNTQRYKALIARSEELMFPGLAEFLEMGGDGICD KCKYRESYGAELSHQFGGVELCSECRLSWRKYLECFVERATKVFPELKTHFEVPV
RuABA3-FL (GenBank No., PQE10596.1) HHHHHHHHHHENLYFQGAGAGAGAGAGMQEVITQTLIDDRFVQLSQQTKNETSKGPG IDDKRWAQEQPNRAKSSDQAAAVTMKAAAPIKEHRDTWYYPPDIASDLQSVNLPAELK GEIFACAWEYTRCVIPNYTNWNRYVAFMRTIIIGVIAEFRGEMVDVTASTSILGYDLDGV LAALFEGTPGHKEMAREYKTFLLITADKASERRDGELFRRYVNALAQSPRHWFRMRDC DALARFTIASALACNDLDDIWYTEEQFEILTEIGDTLYDAVAFYKHRAEGETNSTFAYMP EDLRIKAYSECREILWALDAAWARNPKLVNVINFLRFFGGPIHMMMRRYRFVEENLTIG KSETDKVVDQTRKNFKLWNRVDANKRSIRNTQRYKALIGRSEELMFPGLAEFLEVGGD GVCDKCRYRESYGAEVSHQFGGVELCSECKLSWRQYLECFVERAADVFPELKTYFEV QV
RuABA3 HHHHHHHHHHENLYFQGAGAGAGAGAGDTWYYPPDIASDLQSVNLPAELKGEIFACA WEYTRCVIPNYTNWNRYVAFMRTIIIGVIAEFRGEMVDVTASTSILGYDLDGVLAALFE GTPGHKEMAREYKTFLLITADKASERRDGELFRRYVNALAQSPRHWFRMRDCDALAR FTIASALACNDLDDIWYTEEQFEILTEIGDTLYDAVAFYKHRAEGETNSTFAYMPEDLRIK AYSECREILWALDAAWARNPKLVNVINFLRFFGGPIHMMMRRYRFVEENLTIGKSETDK VVDQTRKNFKLWNRVDANKRSIRNTQRYKALIGRSEELMFPGLAEFLEVGGDGVCDK CRYRESYGAEVSHQFGGVELCSECKLSWRQYLECFVERAADVFPELKTYFEVQV
CiABA3 (GenBank No., KZL82383.1) HHHHHHHHHHENLYFQGAGAGAGAGAGLSLNFIGLLLAFSPYSFMPTFHSIQAKNPAK MSKTPERAPRERDTWYFPPDIAHDLDGIPLPEHVKGEILATAWEYTRTVIPNYTNWKRY VAFMRIVVMGIIAEFKGDLLDVTLGDSVLNYSLDGVLADLFKGTPGHTAMAREYKTFL

LVSGDKSSSRRTGEFFRRYVNVLAYSPTRFFRLRDTDALCRFTIATALACNDLDDVWFT EEQFDLLAEMGDTMYDAVSFFKHRSEGETNSTFAYMPADLRLAAYRQCRELLWALDA AWCTRPETACVTSFLRYFGGPLHLMMRRYRFVEEGLTIGRVEDTEVVNQTRNHFKLW NRIDASLMHANEREKASLERYEAIVRDSEKLLIPGLAEFLEAGGDGHCDSCRYQVSYG ADGEYQFGGVELCEDCRSKWRAFLLSFPERAAKVFPELVGTYNRAITSANNLHSSGDG PSLLVPAA
SkABA3 (GenBank No. WP_051272304.1) HHHHHHENLYFQGAGAGAGAGAGMNFDLNNEQKSITARISDQDQLHYPKEIENDLMN CGLTEKERVEILATAWEYVRCGVPEFTNWEKYIAFVRLTALTTVAEYRGKLVDIDRLLTP GEYVLGYPVRELLDTLFAGTSVYEAMLQEYASCLLFMAEKTRDHQSDLCKKYIEAIASS PSRYYRLRDCDAQVRLFIAAAVACNDLDPDFTEMEYQAMAEIGITLYDAVAFYKHRAE AEVSNLYAYCGQDLEFRQEVYQTARSTLWALETMWCKTVQGRSAINLLKNLPLIHMSM RRYRFVEDGLTIGKPETSAVVRAARNHVKLWYRNDAASNSPAEMERSFESVQYMLYPE LKEALQLPITEMCQKCTRREVYGGVSEEGQFGGVVLCKDSQEEWRHYVRSSESRHLD WLGFLN

*Green fonts, His-tag used for affinity purification with Ni-NTA column; orange fonts, TEV cleavage site; red fonts, $(AG)_5$ linker.

Supplementary Table 2. Oligonucleotides used for site-directed mutagenesis.

Variant	Sequence (5'→3')
BcABA3-F	GGTATGGAACATCAGGATACCTGGTATTATCCTCCG
RuABA3-F	GCGATGACCTGGTACTACCCGCCAGATATTGCG
BcABA3 Y96A-F	GGGAAGCTACCCGTTGTGTTATCCC
BcABA3 I117A-F	GCATCGCCATCATGGGTATCATTGC
BcABA3 I121A-F	CATGGGTGCCATTGCCGAATTTC
BcABA3 E124A-F	TGCCGCATTTCGCGGCG
BcABA3 F167A-F	TAAAACAGCTCTGCTGATCACAGCCG
BcABA3 R202A-F	GTATGGCCGATTGCGATGCC
BcABA3 L207A-F	ATGCCGCAGCCCGCTTTAC
BcABA3 Y242A-F	ACCCTGGCTGATGCAGTTGC
BcABA3 K249A-F	TTATGCACATCGTGCCGAAGGC
BcABA3 H250A-F	TATAAAGCTCGTGCCGAAGGCG
BcABA3 F302A-F	GCTTTGCTGGCGGTCCAATTC
BcABA3 R312A-F	GCGCGCCTATCGCTTTGTTG
BcABA3 Y313A-F	CCGCGCTCGCTTTGTTGAAG

Supplementary Table 3. Crystallization conditions and cryoprotectants of crystals presented in this study.

Dataset	Crystallization condition	Cryoprotectant
Apo-BcABA3	2% Tacsimate (pH 7), 20% (w/v) PEG 3350, 0.1 M HEPES (pH 7.5)	2% Tacsimate (pH 7), 25% (w/v) PEG 3350, 0.1 M HEPES (pH 7.5), 10% glycerol
Apo-RuABA3	20% (w/v) PEG 8000, 0.2 M NaCl, 0.1 M CAPS (pH 10.5)	20% (w/v) PEG 8000, 0.2 M NaCl, 0.1 M CAPS (pH 10.5), 13% ethylene glycol
RuABA3/FsPP	0.2 M sodium malonate (pH 7), 21% (w/v) PEG 3350, 0.1 M Bis-Tris (pH 8.5)	0.2 M sodium malonate (pH 7), 21% (w/v) PEG 3350, 0.1 M Bis-Tris (pH 8.5), 15% glycerol
Apo-SkABA3	10-80 mM $MgCl_2$, 1.3-1.4 M $(NH_4)_2SO_4$, 0.1 M Bis-Tris (pH 6.5)	50 mM $MgCl_2$, 1.4 M $(NH_4)_2SO_4$, 0.1 M Bis-Tris (pH 6.5), 20% glycerol
SkABA3/PPi	0.5 M NaCl, 23% (w/v) PEG 6000 0.1 M Bis-Tris (pH 6.5)	0.5 M NaCl, 23% (w/v) PEG 6000 0.1 M Bis-Tris (pH 6.5), 7% glycerol

Supplementary Table 4. Data collection and refinement statistics for crystal structures

	Apo-BcABA3	Apo-RuABA3	Apo-SkABA3	RuABA3 /FSPP	SkABA3 /PPi
PDB code	8ZAC	8ZAD	8ZAF	8ZAE	8ZAG
Data collection					
Space group	$P2_12_12$	$C222_1$	$C2$	$P2_12_12_1$	$C2$
Unit cell					
a, b, c (Å)	81.2, 166.9, 57.2	68.3, 141.0, 90.3	220.2, 107.8, 81.5	51.8, 89.5, 142.7	86.2, 64.6, 71.0
α, β, γ (°)	90, 90, 90	90, 90, 90	90, 103.7, 90	90, 90, 90	90, 109, 90
Resolution (Å)[a]	25.00-2.45 (2.54-2.45)	36.39-2.10 (2.13-2.10)	25.00-1.96 (2.03-1.96)	35.03-2.28 (2.32-2.28)	25.00-1.60 (1.66-1.60)
No. of observed reflections	29294 (2682)	25866 (1045)	122812 (8751)	27175 (1746)	48426 (4858)
Redundancy	8.5 (6.3)	7.6 (5.8)	3.6 (3.3)	7.3 (4.7)	4.6 (4.5)
Completeness (%)	99.1 (91.9)	99.9 (99.8)	97.9 (96.4)	98.1 (95.0)	99.4 (99.7)
Average I/σ (I)	45.0 (6.1)	10.9 (3.9)	28.2 (2.2)	8.5 (2.0)	47.0 (10.9)
CC 1/2	0.998 (0.981)	0.996 (0.885)	0.997 (0.893)	0.996 (0.792)	0.998 (0.993)
Refinement[c]					
R_{work} (%)	18.4 (24.5)	16.4 (22.0)	19.6 (29.2)	17.7 (27.3)	18.1 (24.6)
R_{free} (%)	25.4 (36.2)	21.2 (26.6)	22.3 (27.4)	24.9 (29.5)	22.4 (29.0)
r.m.s.d. bonds (Å)[d]	0.008	0.010	0.011	0.009	0.013
r.m.s.d. angles (°)	1.521	1.600	1.728	1.569	1.954
Ramachandran statistics[e]					
Most favored (%)	95.4	97.9	98.2	97	98.6
Allowed (%)	4.6	2.1	1.8	3	1.4
Outliers (%)	0	0	0	0	0
Average B-factor (Å^2)					
Protein/atoms	61.2/5794	24.1/2806	46.8/8393	39.1/5451	18.5/2911
Water/ atoms	54.1/209	35.8/375	52.2/660	38.7/317	29.2/374
Ligand/atoms	-	-	61.4/20	61.2/48	20.8/9
Ion/atoms	74.0/2	26.8/1	56.1/3	54.9/4	17.1/3

[a] Values in parentheses are for the highest resolution shell.

[b] $R_{merge} = \Sigma_{hkl}\Sigma i\,|I_i(hkl) - \langle I(hkl)\rangle| / \Sigma_{hkl}\Sigma_i I_i(hkl)$, in which the sum is over all the i measured reflections with equivalent miller indices hkl; $\langle I(hkl)\rangle$ is the averaged intensity of these i reflections, and the grand sum is over all measured reflections in the data set.

[c] All positive reflections were used in the refinement.

[d] According to Engh and Huber[4].

[e] Calculated by using MolProbity[5].

Supplementary Table 5. Partial results of BcABA3 homologous structure searching with DALI server

No.	chain	Z	RMSD	LALI	Nres	% ID	Description
1	5GUE-B	14.8	3.4	227	285	11	Cyclooctat-9-en-7-ol synthase
2	6GGJ-A	14.8	3.5	227	283	11	Cyclooctat-9-en-7-ol synthase
3	7AO2-B	14.8	3.6	227	293	11	Cyclooctat-9-en-7-ol synthase
4	7AO2-A	14.8	3.6	227	293	11	Cyclooctat-9-en-7-ol synthase
5	5GUE-B	14.8	3.4	226	285	11	Cyclooctat-9-en-7-ol synthase
6	5GUE-C	14.8	3.4	226	285	11	Cyclooctat-9-en-7-ol synthase
7	7AO3-B	14.8	3.6	227	293	11	Cyclooctat-9-en-7-ol synthase
8	5GUE-D	14.8	3.4	226	285	11	Cyclooctat-9-en-7-ol synthase
9	7AOL-A	14.7	3.5	226	3.2	11	Cyclooctat-9-en-7-ol synthase
10	6GGJ-B	14.7	3.5	227	296	11	Cyclooctat-9-en-7-ol synthase
11	4OMG-A	14.7	3.5	225	280	10	Geranylgeranyl diphosphate cyclase
12	7AOL-B	14.7	3.5	228	296	11	Cyclooctat-9-en-7-ol synthase
13	7AO0-A	14.7	3.6	227	295	11	Cyclooctat-9-en-7-ol synthase
14	7AO3-A	14.7	3.5	227	303	10	Cyclooctat-9-en-7-ol synthase
15	6GGI-B	14.6	3.5	226	300	11	Cyclooctat-9-en-7-ol synthase
16	6GGI-A	14.6	3.5	226	300	11	Cyclooctat-9-en-7-ol synthase
17	7AO0-B	14.6	3.5	227	296	11	Cyclooctat-9-en-7-ol synthase
18	4OMH-A	14.5	3.4	221	280	10	Geranylgeranyl diphosphate cyclase
19	4OMH-B	14.5	3.4	223	282	9	Geranylgeranyl diphosphate cyclase
20	5IN8-C	14.5	3.8	224	304	11	Aristolochene synthase
21	5IN8-A	14.5	3.6	221	304	11	Aristolochene synthase
22	4OMG-B	14.4	3.5	223	279	10	Geranylgeranyl diphosphate cyclase
23	6GGL-A	14.4	3.4	219	277	10	Cyclooctat-9-en-7-ol synthase
24	5GUC-A	14.4	3.4	222	281	9	Cyclooctat-9-en-7-ol synthase
25	5GUC-B	14.4	3.5	222	281	9	Cyclooctat-9-en-7-ol synthase
26	7AO5-A	14.4	3.4	221	279	10	Cyclooctat-9-en-7-ol synthase
27	5A0K-A	14.4	3.6	224	311	10	Labdane-related diterpene synthase
28	6GGK-B	14.3	3.4	221	277	10	Cyclooctat-9-en-7-ol synthase
29	7AO5-B	14.3	3.4	220	278	10	Cyclooctat-9-en-7-ol synthase
30	4KVI-C	14.3	3.6	224	304	11	Aristolochene synthase
31	5IVG-C	14.3	3.6	221	304	11	Aristolochene synthase
32	4KVD-B	14.3	3.6	224	304	11	Aristolochene synthase
33	4KVI-B	14.3	3.6	221	304	11	Aristolochene synthase
34	5IMI-A	14.3	3.6	224	306	11	Aristolochene synthase
35	5IMI-B	14.3	3.7	224	304	11	Aristolochene synthase
36	5IN8-B	14.3	3.7	225	305	11	Aristolochene synthase
37	4KUX-B	14.3	3.6	221	304	11	Aristolochene synthase
38	5A0J-A	14.3	3.6	222	311	10	Labdane-related diterpene synthase
39	6OH7-A	14.3	3.5	223	311	10	Labdane-related diterpene synthase
40	5A0I-B	14.2	3.5	218	303	9	Labdane-related diterpene synthase

41	6GGL-B	14.2	3.4	220	280	10	Cyclooctat-9-en-7-ol synthase
42	4KUX-C	14.2	3.6	220	304	10	Aristolochene synthase
43	5IMP-C	14.2	3.6	224	304	11	Aristolochene synthase
44	4KWD-B	14.2	3.6	220	304	10	Aristolochene synthase
45	4KVW-C	14.2	3.6	221	304	11	Aristolochene synthase
46	4KVW-B	14.2	3.6	221	304	11	Aristolochene synthase
47	5IMP-A	14.2	3.6	224	304	11	Aristolochene synthase
48	5IMN-A	14.2	3.6	222	304	11	Aristolochene synthase
49	4KUX-A	14.2	3.7	224	304	11	Aristolochene synthase
50	5IMI-D	14.2	3.7	221	306	11	Aristolochene synthase
51	4KVD-D	14.2	3.7	224	304	11	Aristolochene synthase
52	4KWD-D	14.2	3.7	224	304	11	Aristolochene synthase
53	4KVY-D	14.2	3.8	224	304	11	Aristolochene synthase
54	4KVD-C	14.2	3.6	223	304	10	Aristolochene synthase
55	5IVG-B	14.2	3.6	221	304	11	Aristolochene synthase
56	2OA6-D	14.2	3.7	222	306	10	Aristolochene synthase
57	5IMI-C	14.2	3.6	223	304	11	Aristolochene synthase
58	4KVY-C	14.2	3.7	224	304	11	Aristolochene synthase
59	5IVG-A	14.2	3.7	221	305	11	Aristolochene synthase
60	4KVY-B	14.2	3.6	223	304	11	Aristolochene synthase
61	4KWD-A	14.2	3.7	224	304	11	Aristolochene synthase
62	4OKM-A	14.1	4.0	244	346	11	Terpene synthase metal-binding domain-containing protein
63	5IN8-D	14.1	3.6	220	304	11	Aristolochene synthase
64	5IMN-C	14.1	3.6	220	304	11	Aristolochene synthase
65	4KVW-A	14.1	3.8	222	304	10	Aristolochene synthase
66	4KVW-D	14.1	3.7	225	304	11	Aristolochene synthase
67	5IMN-B	14.1	3.7	221	304	10	Aristolochene synthase
68	6OH8-B	14.1	3.5	217	305	9	Aristolochene synthase
69	5IMP-D	14.1	3.7	222	304	10	Aristolochene synthase
70	4KWD-C	14.1	3.7	223	304	10	Aristolochene synthase
71	5IMI-B	14.1	3.8	225	306	11	Aristolochene synthase
72	5IVG-D	14.1	3.7	219	305	11	Aristolochene synthase
73	4OKZ-D	14.0	4.1	241	346	10	Terpene synthase metal-binding domain-containing protein
74	4KVI-A	14.0	3.7	220	304	12	Aristolochene synthase
75	5IMN-D	14.0	3.7	222	304	11	Aristolochene synthase
76	4KVY-A	14.0	3.7	219	304	10	Aristolochene synthase
77	6OH8-A	14.0	3.7	218	306	9	Labdane-related diterpene synthase
78	4OKM-B	13.9	4.1	243	345	11	Terpene synthase metal-binding domain-containing protein
79	4KVI-D	13.9	3.6	217	304	12	Aristolochene synthase
80	4KVD-A	13.9	3.7	220	304	110	Aristolochene synthase

81	4OKZ-A	13.9	4.0	244	346	11	Terpene synthase metal-binding domain-containing protein
82	4KUX-D	13.9	3.8	221	304	11	Aristolochene synthase
83	6GGK-A	13.8	3.4	222	278	11	Cyclooctat-9-en-7-ol synthase
84	4OKZ-C	13.8	4.0	242	345	11	Terpene synthase metal-binding domain-containing protein
85	7AO4-B	13.7	3.4	220	280	11	Cyclooctat-9-en-7-ol synthase
86	7AO4-A	13.7	3.4	218	280	11	Cyclooctat-9-en-7-ol synthase
87	2PS7-B	13.7	3.7	227	350	10	Trichodiene synthase
88	6OH6-A	13.6	3.4	219	311	10	Labdane-related diterpene synthase
89	2PS6-B	13.6	3.8	228	350	10	Trichodiene synthase
90	2Q9Z-B	13.6	3.7	228	353	9	Trichodiene synthase
91	2AET-B	13.6	3.8	229	353	9	Trichodiene synthase
92	2AEL-B	13.6	3.8	228	353	9	Trichodiene synthase
93	7W5I-B	13.6	4.0	227	339	12	Terpene cyclase 6
94	3CKE-A	13.5	3.4	214	295	13	Aristolochene synthase
95	1YYS-B	13.5	3.8	228	351	9	Trichodiene synthase
96	1YYU-B	13.5	3.9	229	354	10	Trichodiene synthase
97	2PS4-B	13.5	3.9	229	354	10	Trichodiene synthase
98	1YYU-A	13.5	3.9	228	354	10	Trichodiene synthase
99	2PS4-A	13.5	3.9	228	354	9	Trichodiene synthase
100	1YYR-A	13.5	4.0	230	353	9	Trichodiene synthase
101	1YYS-A	13.5	4.0	228	353	9	Trichodiene synthase
102	2AEK-B	13.5	4.0	229	354	9	Trichodiene synthase
103	2PS7-A	13.5	3.9	228	354	10	Trichodiene synthase
104	2PS6-A	13.5	3.9	229	352	10	Trichodiene synthase
105	1YYQ-A	13.5	3.9	229	353	9	Trichodiene synthase
106	2PS5-B	13.5	3.7	227	353	9	Trichodiene synthase
107	3BNY-D	13.4	3.5	213	297	12	Aristolochene synthase
108	1JFA-A	13.4	3.9	229	354	10	Trichodiene synthase
109	2AEL-A	13.4	3.9	228	352	9	Trichodiene synthase
110	2AEK-A	13.4	3.9	228	354	9	Trichodiene synthase
111	1TTT-B	13.4	4.0	228	354	11	Trichodiene synthase
112	2PS5-A	13.4	3.9	228	353	10	Trichodiene synthase
113	1JFG-B	13.4	3.8	229	354	10	Trichodiene synthase
114	1YJ4-B	13.4	3.9	226	349	9	Trichodiene synthase
115	1KIZ-A	13.4	4.0	228	354	10	Trichodiene synthase
116	1YYT-A	13.4	3.9	228	354	10	Trichodiene synthase
117	2AET-A	13.4	4.0	229	352	9	Trichodiene synthase
118	1YJ4-A	13.4	3.9	227	354	9	Trichodiene synthase
119	2E4O-C	13.4	3.6	217	296	12	Aristolochene synthase
120	1YYR-B	13.4	3.8	229	352	9	Trichodiene synthase
121	3BNX-C	13.4	3.7	216	295	12	Aristolochene synthase

122	1KIZ-B	13.4	4.0	229	354	10	Trichodiene synthase
123	2OA6-C	13.4	3.7	219	292	12	Aristolochene synthase
124	1JFG-A	13.4	4.0	229	354	9	Trichodiene synthase
125	2PS8-A	13.4	4.0	229	354	10	Trichodiene synthase
126	3BNX-B	13.3	3.4	213	298	12	Aristolochene synthase
127	3BNY-A	13.3	3.4	213	294	12	Aristolochene synthase
128	2OA6-B	13.3	3.5	213	295	13	Aristolochene synthase
129	2E4O-B	13.3	3.6	217	295	12	Aristolochene synthase
130	2E4O-A	13.3	3.6	217	295	12	Aristolochene synthase
131	2E4O-D	13.3	3.5	213	294	12	Aristolochene synthase
132	3CKE-C	13.3	3.4	213	295	12	Aristolochene synthase
133	1KIY-B	13.3	4.0	228	354	11	Trichodiene synthase
134	1KIY-A	13.3	3.9	228	354	11	Trichodiene synthase
135	1JFA-B	13.3	3.9	227	350	9	Trichodiene synthase
136	2Q9Y-B	13.3	3.8	230	352	10	Trichodiene synthase
137	2Q9Y-A	13.3	4.0	228	352	10	Trichodiene synthase
138	2Q9Z-A	13.3	4.0	228	354	10	Trichodiene synthase
139	7OC4-A	13.3	3.9	218	389	11	Alpha-humulene synthase ASR6
140	3BNX-A	13.3	3.4	214	296	13	Aristolochene synthase
141	3CKE-B	13.3	3.4	213	297	12	Aristolochene synthase
142	3BNY-C	13.2	3.4	210	293	12	Aristolochene synthase
143	7W5F-A	13.2	3.9	228	339	13	Terpene cyclase 6
144	7W5F-B	13.2	4.0	228	338	11	Terpene cyclase 6
145	1YYQ-B	13.2	3.8	229	351	10	Trichodiene synthase
146	2PS8-B	13.2	3.7	228	354	10	Trichodiene synthase
147	1DGP-B	13.2	3.5	212	290	12	Aristolochene synthase
148	6LCC-B	13.2	3.9	227	374	10	AaTPS
149	4ZQ8-B	13.2	3.6	227	321	10	Isoprenoid synthase
150	4ZQ8-A	13.1	3.6	222	320	10	Isoprenoid synthase

Supplementary Table 6. Atomic absorption spectrometric analyses

Protein	Ion	Concentration (mg mL^{-1})	
		Duplicate-1	Duplicate-2
BcABA3	Mg	0.074	0.067
	Ni	0.025	0.023
	Zn	0.221	0.213
RuABA3	Mg	UD*	UD*
	Ni	0.021	0.017
	Zn	0.183	0.183
SkABA3	Mg	0.038	UD*
	Ni	0.011	0.013
	Zn	0.288	0.315

*UD, undetectable

Supplementary Table 7. BcABA3 homologue sequences used in **Supplementary Fig. 12**

No.	Source	GenBank accession number	Sequence identity to BcABA3
1	*Botrytis cinerea*	XP_024550392.1	100%
2	*Rutstroemia* sp.	PQE10596.1	86.2%
3	*Pseudogymnoascus* sp. WSF 3629	OBT40576.1	59.1%
4	*Leptosphaeria maculans* JN3	XP_003843016.1	57.5%
5	*Amycolatopsis mediterranei*	WP_013229565.1	54.1%
6	*Pseudogymnoascus*_sp. VKM F-4518 (FW-2643)	KFZ0018.1	54.3%
7	*Colletotrichum higginsianum* IMI 349063	XP_018158055.1	52.8%
8	*Aspergillus niger*	GAQ47445.1	52.8%
9	*Eutypa lata* UCREL1	EMR65886.1	52.4%
10	*Exophiala xenobiotica*	XP_013319909.1	51.6%
11	*Aureobasidium subglaciale*	KAI5241785.1	51%
12	*Elsinoe australis*	PSK60221.1	50.3%
13	*Mycena galopus*	KAF8182497.1	48.8%
14	*Pyrenophora seminiperda*	RMZ73257.1	48.6%
15	*Alternaria alternata*	XP_018379073.1	47.3%
16	*Fusarium redolens*	XP_046043392.1	44.3%
17	*Stemphylium lycopersici*	KNG44597.1	44.2%
18	*F. oxysporum* f. sp. raphani 54005	EXK82261.1	43.8%
19	*Streptomyces* sp. NRRL F-6131	WP_030303341.1	42.6%
20	*Shimazuella kribbensis*	WP_051272304.1	36.3%

Supplementary References

1. Takino, J., *et al*. Unveiling biosynthesis of the phytohormone abscisic acid in Fungi: unprecedented mechanism of core scaffold formation catalyzed by an unusual sesquiterpene synthase. *J. Am. Chem. Soc.* **140**, 12392-12395 (2018).

2. McWilliam, H., *et al*. Analysis tool web services from the EMBL-EBI. *Nuc. Acids Res.* **41**, W597-W600 (2013).

3. Robert, X., & Gouet, P. Deciphering key features in protein structures with the new ENDscript server. *Nuc. Acids Res*. **42**, W320-W324 (2014).

4. Engh, RA., & Huber, R. Accurate bond and angle parameters for X-ray protein structure refinement. *Acta Crystallogr. A* **47**, 392-400 (1991).

5. Chen, VB., et al. MolProbity: all-atom structure validation for macromolecular crystallography. *Acta Crystallogr. D: Biol Crystallogr.* **66**, 12-21 (2010).